LETTER

doi:10.1038/nature17955

A shared neural ensemble links distinct contextual memories encoded close in time

Denise J. Cai[1]*, Daniel Aharoni[1,2,3]*, Tristan Shuman[2,3]*, Justin Shobe[1]*, Jeremy Biane[4,5], Weilin Song[1], Brandon Wei[1], Michael Veshkini[1], Mimi La-Vu[1], Jerry Lou[2,3], Sergio E. Flores[2,3], Isaac Kim[1], Yoshitake Sano[1], Miou Zhou[1], Karsten Baumgaertel[6], Ayal Lavi[1], Masakazu Kamata[7], Mark Tuszynski[4,5], Mark Mayford[6], Peyman Golshani[2,3] & Alcino J. Silva[1]

Recent studies suggest that a shared neural ensemble may link distinct memories encoded close in time[1–12]. According to the memory allocation hypothesis[1,2], learning triggers a temporary increase in neuronal excitability[13–15] that biases the representation of a subsequent memory to the neuronal ensemble encoding the first memory, such that recall of one memory increases the likelihood of recalling the other memory. Here we show in mice that the overlap between the hippocampal CA1 ensembles activated by two distinct contexts acquired within a day is higher than when they are separated by a week. Several findings indicate that this overlap of neuronal ensembles links two contextual memories. First, fear paired with one context is transferred to a neutral context when the two contexts are acquired within a day but not across a week. Second, the first memory strengthens the second memory within a day but not across a week. Older mice, known to have lower CA1 excitability[15,16], do not show the overlap between ensembles, the transfer of fear between contexts, or the strengthening of the second memory. Finally, in aged mice, increasing cellular excitability and activating a common ensemble of CA1 neurons during two distinct context exposures rescued the deficit in linking memories. Taken together, these findings demonstrate that contextual memories encoded close in time are linked by directing storage into overlapping ensembles. Alteration of these processes by ageing could affect the temporal structure of memories, thus impairing efficient recall of related information.

Contextual memories are encoded in discrete and sparse populations of neurons in the hippocampus[17–21]. Recent findings demonstrated that increasing the relative neuronal excitability of a subset of neurons increases the probability that those neurons will participate in a memory trace[6,8–11]. While previous studies used viral vectors to manipulate excitability, temporary increases in excitability occur naturally following learning, including in the hippocampus[13,14,22]. Therefore, two distinct memories could be linked across time because the temporary increase in excitability would bias the storage of a subsequent memory to many of the same neurons that encoded the first memory, such that recall of one of these events would also probably lead to recall of the other, a key prediction of the memory allocation hypothesis[1,2].

To investigate the neuronal ensembles encoding multiple memories, we constructed an open-source, head-mounted, miniature fluorescent microscope[7,23], to image *in vivo* calcium transients in CA1 neurons using GCaMP6f. With this approach we tracked the activation of the same neurons in mice as they freely explored three distinct novel contexts across multiple days (Fig. 1a–c, Extended Data Figs 1 and 2). We recorded CA1 neurons activated by three different contexts separated by either 5 h or 7 days. Previous studies show transient learning-dependent increases in neuronal excitability[13,14,24] and we confirmed that 5 h after context exposure there was an increase in excitability in CA1 neurons that encoded the context (Extended Data Fig. 3c, d). Therefore, we predicted that the overlap between the neural representations of two contexts separated by 5 h would be higher than the overlap of the neural representations of two contexts separated by 7 days.

We exposed mice to three distinct, novel contexts. A and C were separated by 7 days; B and C were separated by 5 h. Using miniature microscopes, we imaged active CA1 neurons during each context exploration (Fig. 1d). We found more overlap between the neural ensembles encoding B and C, spaced 5 h apart, than between the neural ensembles encoding A and C, spaced 7 days apart (Fig. 1f, Extended Data Fig. 4a, b). Notably, this difference was not due to differences in the total number of active CA1 cells in the three contexts (Fig. 1e). We confirmed these findings with the TetTag transgenic system, a non-invasive technique that allowed us to tag neurons active during the exploration of two contexts[25,26] (Fig. 2a, b, Extended Data Fig. 3a, b). We used this transgenic approach to tag the neural ensemble activated by exploration of an initial novel context (GFP^+) and compared this population to the ensemble activated by exploration of a second distinct, novel context (using ZIF immunohistochemistry), either 5 h or 7 days later (Fig. 2c–e). When the two contexts were separated by 7 days, the overlap between the two ensembles was similar to what was expected due to chance (Fig. 2f), indicating that independent populations of neurons encoded the two distinct contexts. However, when the two contexts were separated by 5 h, overlap between neuronal ensembles was significantly above chance levels and higher than in the 7 days group (Fig. 2f). Together, the calcium imaging and TetTag data provide converging evidence that overlapping neural ensembles encode distinct contexts when these contexts are separated by 5 h, but not by 7 days.

To determine whether the overlap of neuronal representations link contextual memories that occurred close in time, such that the recall of one is more likely to lead to the recall of the other, we again exposed animals to three distinct contexts as described above: A and C were separated by 7 days, and B and C were separated by 5 h. Two days later, mice were placed in C and given an immediate footshock (Fig. 3a). Since the neural representations of B and C overlap more than A and C (Extended Data Fig. 5), recall of C (shocked context) should lead to recall of B (but not A). Therefore, the fear associated with C should transfer to B (but not to A). Remarkably, we found that mice tested in B, a context in which they had not been shocked, froze as much as mice tested in C (shocked context; Fig. 3b). In contrast, mice tested in A froze significantly less than mice tested in the other two contexts.

[1]Departments of Neurobiology, Psychiatry & Biobehavioral Sciences and Psychology, Integrative Center for Learning and Memory, Brain Research Institute, University of California, Los Angeles, California 90095, USA. [2]Departments of Neurology and Psychiatry & Biobehavioral Sciences, Integrative Center for Learning and Memory, Brain Research Institute, University of California, Los Angeles, California 90095, USA. [3]West Los Angeles VA Medical Center, 11301 Wilshire Blvd, Los Angeles, California 90073, USA. [4]Department of Neurosciences, University of California, San Diego, La Jolla, California 92093, USA. [5]Veterans Affairs Medical Center, San Diego, California 92161, USA. [6]Departments of Cell Biology and Neurosciences, Institute for Childhood and Neglected Diseases, The Scripps Research Institute, 10550 North Torrey Pines Road, La Jolla, California 92037, USA. [7]Division of Hematology/Oncology, David Geffen School of Medicine, University of California, Los Angeles, California 90095, USA.
*These authors contributed equally to this work.

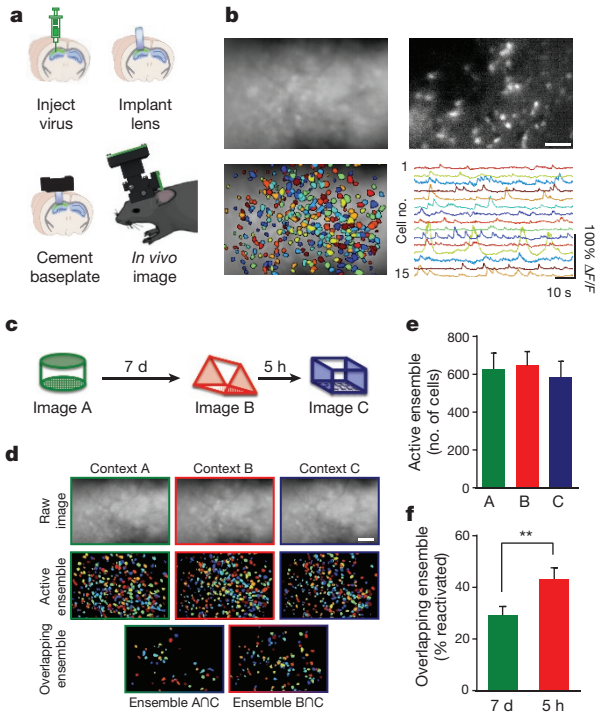

Figure 1 | Calcium imaging CA1 with integrated miniature microscopes while exploring different contexts. a, A microendoscope was implanted directly above CA1 expressing viral GCaMP6f and a baseplate was affixed onto the skull. A miniature fluorescent wide-field microscope was used to image CA1 neurons across repeated imaging sessions. **b**, Top left, example image of mean fluorescence during context exploration. Top right, example image of relative fluorescent change ($\Delta F/F$). Bottom left, cells extracted from $\Delta F/F$. Scale bar represents 100 μm. Bottom right, example traces of $\Delta F/F$ colour coded to represent individual neurons. **c**, Experimental design. Mice were imaged while exploring three novel contexts (A, B, C) separated by 7 days or 5 h. **d**, Representative imaging during context exploration. Top row, images of mean fluorescence from each session. Middle row, ensemble of cells active in each session. Bottom row, cells that were active in two sessions. Scale bar represents 100 μm. **e**, There was no difference in the number of cells active across the three context explorations (one-way, repeated measures ANOVA, $F_{2,7} = 2.14$, not significant, $n = 8$ mice). **f**, There was an increase in the overlapping ensemble when contexts are separated by 5 h compared to 7 days (paired t-test, $t_7 = 3.830$, $P = 0.0065$, $n = 8$). $^{**}P < 0.01$. Results show mean ± s.e.m.

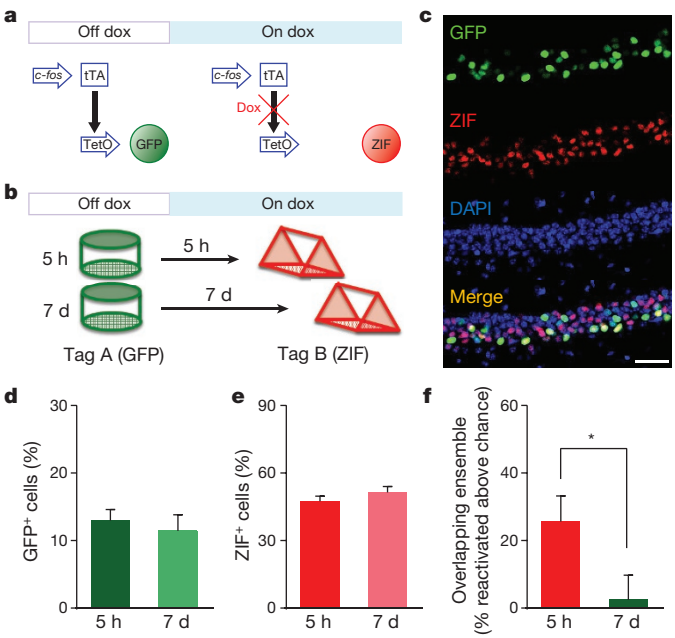

Figure 2 | Tagging neural ensembles of contextual memories with the TetTag system. a, Schematic design of the TetTag system. Dox, doxycycline; tTA, tetracycline-transactivator; TetO, tetracycline response element. **b**, Experimental design. Cells active in context A were tagged with GFP and cells active in context B, either 5 h or 7 days later, were labelled with ZIF immunohistochemistry. **c**, Representative examples of GFP, ZIF, DAPI and merged images of CA1. Scale bar represents 50 μm. **d**, There was no difference between the percentage of cells positive for GFP (unpaired t-test, $t_{24} = 0.54$, not significant, $n = 15$, 11 mice). **e**, There was no difference between the percentage of cells positive for ZIF (unpaired t-test, $t_{24} = 1.11$, not significant, $n = 15$, 11 mice). **f**, There was an increase in the overlapping ensemble between contexts when spaced 5 h apart compared to 7 days apart (unpaired t-test, $t_{24} = 2.15$, $P = 0.0422$, $n = 15$, 11 mice). The level of the overlapping ensemble for the 5 h group was above chance (one-sample t-test against 0, $t_{14} = 3.402$, $P = 0.0043$) and at chance for the 7 day group (one-sample t-test against 0, $t_{10} = 0.323$, not significant). $^{*}P < 0.05$. Results show mean ± s.e.m.

These results support the hypothesis that the overlap between neuronal representations contextually links memories close in time.

Next, we tested whether the memories for B and C remain distinct, rather than forming a unitary memory. If so, extinction of the fear associated with B should not affect recall in C. Again, we exposed animals to B and 5 h later to C, and then two days later paired C with a footshock. Two days after the footshock, the mice were tested in either C (shocked context), B (5 h; not shocked), or D (novel context; Fig. 3c). Consistent with the prior experiment, mice froze similarly in C and B, despite never having been shocked in B. However, they froze less in a novel context (D; Fig. 3d, Extended Data Fig. 6b), demonstrating memory specificity. Next, we carried out repeated exposures in either context C, B, or D daily for 5 days. On the final day, the mice were tested in C (shocked context). As expected, repeated exposures in C (compared to repeated exposures in novel context D) resulted in lower freezing during the extinction test (Fig. 3e). Mice that were repeatedly exposed to B did not show less freezing in C, demonstrating that repeated exposures in B do not cause extinction in C. These results demonstrate that although the memories for B and C show considerable overlap in their ensembles, and recall of B appears to trigger recall of C, memories for these two contexts, acquired 5 h apart, remain distinct.

Recent findings demonstrated that manipulations that enhance neuronal excitability can lead to increases in memory strength[11]. We found that 5 h after exposure to a context, there was an increase in excitability in cells that encoded that context (Extended Data Fig. 3c, d). Thus, the sharing of the neural ensemble and the increase in excitability should result in the strengthening of the memory for a second context 5 h later. To test for modulation of memory strength, mice were exposed to B and then exposed to C 5 h or 7 days later. Two days later, animals received an immediate shock in C. Two days after that, they were tested in C. Home cage controls were trained in the same manner, except they were not exposed to B (Fig. 3f). Mice trained with the 5 h interval had enhanced memory for C compared to either mice trained with the 7 day interval or home cage controls (Fig. 3g; Extended Data Figs 6c, d and 7). Furthermore, this enhancement required NMDA-receptor activity (Extended Data Fig. 8). These data support our previous findings and indicate that for a period of time (5 h, but not 7 days) the processes triggered by the encoding of one memory can modulate the strength of subsequent memories.

Taken together, the results presented above demonstrate that the overlap between the neuronal ensembles representing two separate contextual memories leads to linking of these memories and suggests that excitability has a key role in this process. Since CA1 neuronal excitability decreases with ageing[15,16,22,27], we predicted that memory-linking processes may be disrupted in older mice. To test this, we started by repeating the calcium imaging (Fig. 4a) as well as the TetTag experiment (Extended Data Fig. 9e, f) in aged mice. Unlike in young adult mice (3–6 months old), in aged mice (14–18 months old) there

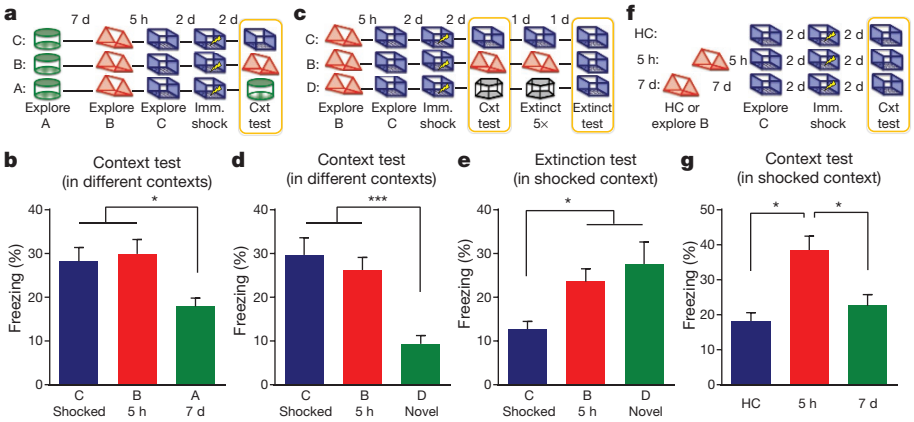

Figure 3 | Memories are contextually linked but distinct. a, Design for transfer of fear experiment. Imm. shock, immediate shock; cxt test, context test. **b**, There was a significant difference in freezing between groups that were tested in different contexts (A, B, C) for the transfer of fear experiment (one-way ANOVA, $F_{2,47} = 4.62$, $P = 0.01$, $n = 18, 17, 15$ mice). There was no difference between freezing in contexts C and B ($t_{45} = 0.42$, not significant). Animals had less freezing in context A than C ($t_{47} = 2.46$, $P = 0.02$) and B ($t_{47} = 2.83$, $P = 0.007$). **c**, Design for extinction experiment. **d**, There was a significant difference in freezing during the context test (one-way ANOVA, $F_{2,57} = 12.99$, $P < 0.0001$, $n = 20, 20, 20$ mice). There was no difference between freezing in contexts C and B ($t_{57} = 0.80$, not significant). Animals had less freezing in context D than C ($t_{57} = 4.76$, $P < 0.0001$) and B ($t_{57} = 3.96$, $P = 0.0002$). **e**, There was a significant difference in freezing during the extinction test (one-way ANOVA, $F_{2,57} = 4.79$, $P = 0.01$, $n = 20, 20, 20$ mice). There were no differences in freezing between groups B and D ($t_{57} = 0.81$, not significant). Group C had less freezing than groups B ($t_{57} = 2.18$, $P = 0.03$) and D ($t_{57} = 2.99$, $P = 0.004$). **f**, Design for enhancement experiment. **g**, There was a significant difference in freezing in the enhancement experiment (one-way ANOVA, $F_{2,51} = 9.63$, $P < 0.001$, $n = 14, 20, 20$ mice). The 5 h group had more freezing than the home cage (HC) ($t_{51} = 3.98$, $P = 0.0002$) and 7 day ($t_{51} = 3.45$, $P = 0.001$) groups. There was no difference between home cage or 7 d groups ($t_{51} = 0.86$, not significant). $^*P < 0.05$, $^{**}P < 0.01$. Results show mean ± s.e.m.

was no difference between the overlap of neural ensembles encoding contexts spaced 5 h or 7 days apart (Fig. 4b). This lack of overlap was not due to an inability to reliably reactivate the same neural ensemble during recall of the same context (Extended Data Fig. 9a, b) or to general contextual memory deficits (Extended Data Fig. 9c, d).

The results presented above predict that the lack of a shared neural representation in aged mice should disrupt memory linking. To test this hypothesis, we repeated in aged mice the experiment testing the transfer of fear between contexts (Fig. 4c). The results showed that the fear associated with C does not transfer to B in aged mice: the freezing triggered by B (no shock context) was not different than that observed in a novel context, D, and significantly lower than that in C (shocked context; Fig. 4d). Similarly, we found that, unlike in young mice, in aged mice exposure to B (5 h before exposure to C) does not enhance memory for C (Fig. 4e, f). Importantly, this was not due to a deficit in learning of a single context, since when trained with a single context the performance of aged mice was indistinguishable from that of young mice (Extended Data Fig. 9c, d). Furthermore, the differences between young and aged mice were also not due to strain differences, as we replicated the transfer and enhancement experiments with young mice from the same genetic background as the aged mice (Extended Data Fig. 6). Altogether, these results strongly support the role of neuronal excitability in linking distinct contextual memories encoded close in time, as aged mice exposed to two contexts close in time did not show the increased overlap between ensembles which presumably led to the lack of both the transfer of fear between contexts and the strengthening of the second memory.

To increase neuronal excitability and rescue the memory-linking deficit in aged mice, we injected a lentivirus to express hM3Dq designer receptors exclusively activated by designer drugs (DREADD) tagged

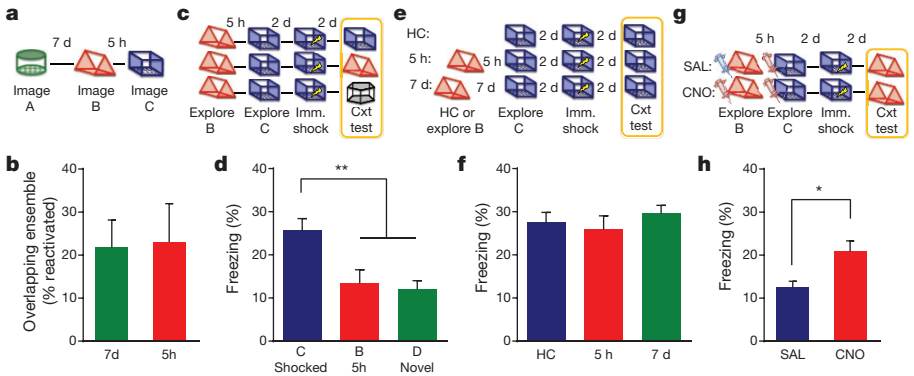

Figure 4 | Age-related deficits in memory linking are rescued by ensemble activation. a, Design for calcium imaging with miniature microscope in aged mice. **b**, There was no difference in the overlapping ensemble between the 5 h and 7 day groups (paired *t*-test, $t_3 = 0.367$, not significant, $n = 4$). **c**, Design for transfer of fear experiment. **d**, There was a significant difference in freezing during the context test (one-way ANOVA, $F_{2,47} = 8.083$, $P = 0.001$, $n = 19, 15, 16$ mice). There was no difference between freezing levels in contexts B and D ($t_{47} = 0.35$, not significant). Animals had more freezing in context C than B ($t_4 = 3.19$, $P = 0.0025$) and D ($t_{47} = 3.619$, $P = 0.0007$). **e**, Design for behavioural enhancement experiment. **f**, There was no difference in freezing between groups (one-way ANOVA, $F_{2,39} = 0.453$, not significant, $n = 15$, 15, 12 mice). **g**, Design for memory linking rescue by activating cells with DREADD receptors. **h**, There was higher freezing in the CNO group compared to the saline-injected (SAL) group (unpaired *t*-test, $t_{31} = 2.36$, $P = 0.02$, $n = 12, 21$ mice). $^*P < 0.05$, $^{**}P < 0.01$. Results show mean ± s.e.m.

with GFP in a sparse population of dorsal CA1 neurons (Extended Data Fig. 10a, b). Clozapine-*N*-oxide (CNO) increases excitability and activates cells that express the DREADD receptors[11] (Extended Data Fig. 10c, d). To bias the allocation of the two contextual memories so that they shared an overlapping neural ensemble, we injected CNO before both learning experiences, spaced 5 h apart (Fig. 4g). The control group was given a saline injection before the first exploration and a CNO injection before the second exploration. To test the behavioural consequences of sharing a neural ensemble, mice were brought back two days later for an immediate shock in the second context. Two days later, mice were tested in the first (non-shocked) context to assess their transfer of fear. The CNO group froze more than the saline-injected group in the non-shocked context (Fig. 4h). This was not due to increased anxiety caused by CNO (Extended Data Fig. 10e, f). Thus, increasing neuronal excitability in aged mice rescued the memory-linking deficit.

Mechanisms that link memories are critically important for organizing the enormous number of related memories stored throughout a lifetime. Our results support the memory allocation hypothesis[1,2] and are consistent with human data and computational modelling[28], suggesting that memories encoded within close temporal proximity are more likely to be co-recalled than memories encoded across more distant time frames. Our data indicate that overlapping populations of CA1 neurons serve to link and strengthen memories, thus facilitating integrated recall of experiences encoded close in time while separating those encoded further in time. Temporary increases in excitability[13–15] probably represent one of a family of mechanisms (synaptic tagging and capture[2,29] is another example) that structure the acquisition and storage of information to facilitate future use and recall. Alteration of these processes, such as decreases in neuronal excitability during ageing, could affect the organization of memory thus impairing efficient recall of related information.

Online Content Methods, along with any additional Extended Data display items and Source Data, are available in the online version of the paper; references unique to these sections appear only in the online paper.

Received 12 January; accepted 24 March 2016.
Published online 23 May 2016.

1. Silva, A. J., Zhou, Y., Rogerson, T., Shobe, J. & Balaji, J. Molecular and cellular approaches to memory allocation in neural circuits. *Science* **326,** 391–395 (2009).
2. Rogerson, T. *et al.* Synaptic tagging during memory allocation. *Nat. Rev. Neurosci.* **15,** 157–169 (2014).
3. Mankin, E. A. *et al.* Neuronal code for extended time in the hippocampus. *Proc. Natl Acad. Sci. USA* **109,** 19462–19467 (2012).
4. Han, J.-H. *et al.* Neuronal competition and selection during memory formation. *Science* **316,** 457–460 (2007).
5. Han, J.-H. *et al.* Selective erasure of a fear memory. *Science* **323,** 1492–1496 (2009).
6. Zhou, Y. *et al.* CREB regulates excitability and the allocation of memory to subsets of neurons in the amygdala. *Nat. Neurosci.* **12,** 1438–1443 (2009).
7. Ziv, Y. *et al.* Long-term dynamics of CA1 hippocampal place codes. *Nat. Neurosci.* **16,** 264–266 (2013).
8. Epsztein, J., Brecht, M. & Lee, A. K. Intracellular determinants of hippocampal CA1 place and silent cell activity in a novel environment. *Neuron* **70,** 109–120 (2011).
9. Lee, D., Lin, B. J. & Lee, A. K. Hippocampal place fields emerge upon single-cell manipulation of excitability during behavior. *Science* **337,** 849–853 (2012).
10. Dragoi, G. & Tonegawa, S. Preplay of future place cell sequences by hippocampal cellular assemblies. *Nature* **469,** 397–401 (2011).
11. Yiu, A. P. *et al.* Neurons are recruited to a memory trace based on relative neuronal excitability immediately before training. *Neuron* **83,** 722–735 (2014).
12. Ezzyat, Y. & Davachi, L. What constitutes an episode in episodic memory? *Psychol. Sci.* **22,** 243–252 (2011).
13. Moyer, J. R., Jr, Thompson, L. T. & Disterhoft, J. F. Trace eyeblink conditioning increases CA1 excitability in a transient and learning-specific manner. *J. Neurosci.* **16,** 5536–5546 (1996).
14. McKay, B. M., Matthews, E. A., Oliveira, F. A. & Disterhoft, J. F. Intrinsic neuronal excitability is reversibly altered by a single experience in fear conditioning. *J. Neurophysiol.* **102,** 2763–2770 (2009).
15. Oh, M. M., Oliveira, F. A. & Disterhoft, J. F. Learning and aging related changes in intrinsic neuronal excitability. *Front. Aging Neurosci.* **2,** 2 (2010).
16. Kaczorowski, C. C. & Disterhoft, J. F. Memory deficits are associated with impaired ability to modulate neuronal excitability in middle-aged mice. *Learn. Mem.* **16,** 362–366 (2009).
17. Garner, A. R. *et al.* Generation of a synthetic memory trace. *Science* **335,** 1513–1516 (2012).
18. Guzowski, J. F., McNaughton, B. L., Barnes, C. A. & Worley, P. F. Environment-specific expression of the immediate-early gene *Arc* in hippocampal neuronal ensembles. *Nat. Neurosci.* **2,** 1120–1124 (1999).
19. Liu, X. *et al.* Optogenetic stimulation of a hippocampal engram activates fear memory recall. *Nature* **484,** 381–385 (2012).
20. McKenzie, S. *et al.* Hippocampal representation of related and opposing memories develop within distinct, hierarchically organized neural schemas. *Neuron* **83,** 202–215 (2014).
21. Deng, W., Mayford, M. & Gage, F. H. Selection of distinct populations of dentate granule cells in response to inputs as a mechanism for pattern separation in mice. *eLife* **2,** e00312 (2013).
22. Disterhoft, J. F. & Oh, M. M. Alterations in intrinsic neuronal excitability during normal aging. *Aging Cell* **6,** 327–336 (2007).
23. Ghosh, K. K. *et al.* Miniaturized integration of a fluorescence microscope. *Nat. Methods* **8,** 871–878 (2011).
24. Disterhoft, J. F. & Oh, M. M. Learning, aging and intrinsic neuronal plasticity. *Trends Neurosci.* **29,** 587–599 (2006).
25. Reijmers, L. G., Perkins, B. L., Matsuo, N. & Mayford, M. Localization of a stable neural correlate of associative memory. *Science* **317,** 1230–1233 (2007).
26. Tayler, K. K., Tanaka, K. Z., Reijmers, L. G. & Wiltgen, B. J. Reactivation of neural ensembles during the retrieval of recent and remote memory. *Curr. Biol.* **23,** 99–106 (2013).
27. Murphy, G. G., Shah, V., Hell, J. W. & Silva, A. J. Investigation of age-related cognitive decline using mice as a model system: neurophysiological correlates. *Am. J. Geriatr. Psychiatry* **14,** 1012–1021 (2006).
28. Sederberg, P. B., Howard, M. W. & Kahana, M. J. A context-based theory of recency and contiguity in free recall. *Psychol. Rev.* **115,** 893–912 (2008).
29. Redondo, R. L. & Morris, R. G. Making memories last: the synaptic tagging and capture hypothesis. *Nat. Rev. Neurosci.* **12,** 17–30 (2011).

Acknowledgements We thank B. Khakh for support in the development of the miniaturized microscopes. We thank E. Thai, D. Tarzi, A. Ahuja, K. Lew, E. Lu, E. Stuart, S. Zhang, S. Ghiaee, C. Yang, A. Fariborzi, K. Cheng, N. Rao, A. Chang, C. Grimmick and M. Einstein for help with experiments; N. Rao for assistance with graphical design; and all members of the Silva laboratory for their support. This work was supported by National Institute on Aging R37 AG013622 and the Dr. Miriam and Sheldon G. Adelson Medical Research Foundation to A.J.S.; National Institutes of Health RO1 MH101198, 1U54 HD087101 and VA Merit Award BX00152401A1 to P.G.; National Research Service Award F32 MH97413 and Behavioral Neuroscience Training Grant T32 MH15795 to D.J.C.; Neurobehavioral Genetics Training Grant T32 NS048004 and Neural Microcircuits Training Grant T32 NS058280 to D.A.; Cellular Neurobiology Training Grant T32 NS710133 and Epilepsy Foundation Postdoctoral Research Training Fellowship to T.S.; National Institutes of Health U01 NS094286-01 and David Geffen School of Medicine Dean's Fund for development of open-source miniaturized microscopes to A.J.S. and P.G.

Author Contributions D.J.C., J.S., T.S., D.A. and A.J.S. contributed to the study design. D.A., T.S., D.J.C., P.G. and A.J.S. developed the miniature microscope system. D.A. engineered hardware and software associated with the miniature microscope and wrote the MATLAB analysis suite. T.S., D.J.C., W.S., J.S., S.E.F., J.L. and I.K. performed surgeries. D.J.C., T.S., M.L., W.S. and B.W. conducted calcium imaging and TetTag experiments. M.M. engineered and provided TetTag mice. D.J.C., J.S., T.S., M.L., W.S., B.W., M.V. and M.Z. conducted behavioural experiments. D.J.C., D.A., T.S. and A.L. analysed the data. J.B., D.J.C. and T.S. conducted *in vitro* physiology experiments. M.T. supported physiology experiments. Y.S. and M.K. made DREADD virus. D.J.C., I.K., B.W. and K.B. managed the mouse colony. D.J.C., T.S., D.A., J.S. and A.J.S. wrote the paper. All authors discussed and commented on the manuscript.

Author Information Reprints and permissions information is available at www.nature.com/reprints. The authors declare no competing financial interests. Readers are welcome to comment on the online version of the paper. Correspondence and requests for materials should be addressed to A.J.S. (silvaa@mednet.ucla.edu) or P.G. (pgolshani@mednet.ucla.edu).

METHODS

Subjects. All experimental protocols were approved by the Chancellor's Animal Research Committee of the University of California, Los Angeles, in accordance with NIH guidelines. Adult C57Bl/6NTac, C57Bl/6NTac × 129S6/SvEvTac and C57Bl/6NIA male mice were singly housed on a 12 h light/dark cycle. Young adult mice were 3–6 months old, and aged adult mice were 14–18 months old. TetTag mice were generated by crossing transgenic mice that express a histone 2B–GFP fusion protein controlled by the tetO promoter (strain Tg(tetO-HIST1H2BJ/GFP) 47Efu/J; stock number 005104; Jackson Laboratory) with mice that express tetracycline-transactivator (tTA) protein under control of the *c-fos* (also known as *Fos*) promoter. TetTag mice were maintained in a C57BL/6N background. Mice were born and raised on doxycycline (dox) chow (40 mg kg^{-1}) to prevent GFP expression before experimental manipulations. To open the window for activity-dependent labelling, dox chow was replaced with regular chow for 3 days before the start of an experiment. Expression of new GFP was shut off by administration of high dox chow (1 g kg^{-1}). Memory linking (transfer of fear and enhancement) experiments were conducted with both C57Bl/6NTac × 129S6/SvEvTac and C57Bl/6NIA mice.

Viral construct. AAV1.Syn.GCaMP6f.WPRE.SV40 virus (titre: 4.65×10^{13} GC per ml) was purchased from Penn Vector Core. The hM3Dq vector was derived from the CaMK2a.hM4Di.T2A.EGFP/CREB plasmid[30]. The hM4Di.T2A.EGFP/CREB in that plasmid was replaced by hM3Dq.T2A.EGFP/dTomato. The HA-tagged hM3Dq and dTomato-tagged EGFP are expressed under the CaMK2a promoter and cloned on either side of a T2A self-processing viral peptide. Vesicular-stomatitis-virus-G-protein-pseudotyped lentiviral vectors were produced by calcium-phosphate-mediated transient transfection of human embryonic kidney 293 T (HEK293T) cells, as previously described[30]. Lentivirus vectors were titred on HEK293T cells based on EGFP expression (titre: 6×10^5 cells per ml).

Surgery. Mice were anaesthetized with 1.5 to 2.0% isoflurane for surgical procedures and placed into a stereotactic frame (David Kopf Instruments, Tujunga, CA). Lidocaine (2%; Akorn, Lake Forest, Illinois) was applied to the sterilized incision site as an analgesic, while subcutaneous saline injections were administered throughout each surgical procedure to prevent dehydration. In addition, carprofen (5 mg kg^{-1}) and dexamethasone (0.2 mg kg^{-1}) were administered both during surgery and for 7 days post-surgery with amoxicillin.

For calcium imaging experiments, mice underwent two separate surgical procedures. First, mice were unilaterally microinjected with 500 nl of AAV1.Syn.GCaMP6f.WPRE.SV40 virus at 50 nl min^{-1} into the dorsal CA1 using the stereotactic coordinates: −2.1 mm posterior to bregma, 2.0 mm lateral to midline and −1.65 mm ventral to skull surface. Two weeks later, the microendoscope (a gradient refractive index lens) was implanted above the previous injection site. For the procedure, a 2.0 mm diameter circular craniotomy was centred 0.5 mm medial to the virus injection site. Artificial cerebrospinal fluid (ACSF) was repeatedly applied to the exposed tissue to prevent drying. The cortex directly below the craniotomy was aspirated with a 27-gauge blunt syringe needle attached to a vacuum pump. The microendoscope (0.25 pitch, 0.50 NA, 2.0 mm in diameter and 4.79 mm in length, Grintech Gmbh) was slowly lowered with a stereotaxic arm above CA1 to a depth of 1.35 mm ventral to the surface of the skull at the most posterior point of the craniotomy. Next, a skull screw was used to anchor the microendoscope to the skull. Both the microendoscope and skull screw were fixed with cyanoacrylate and dental cement. Kwik-Sil (World Precision Instruments) covered the microendoscope. Two weeks later, a small plastic baseplate was cemented onto the animal's head atop the previously formed dental cement. Debris was removed from the exposed lens with double-distilled H_2O, lens paper and forceps. The microscope was placed on top of the baseplate and locked in a position in which the field of focus was in view, so that cells and visible landmarks, such as blood vessels, appeared sharp and in focus. Finally, a plastic cover was fit into the baseplate and secured by magnets.

For aged DREADD experiments, mice were bilaterally microinjected with 700 nl of lentivirus CaMK2.hM3Dq.T2A.EGFP/dTomato virus at 100 nl min^{-1} into the dorsal CA1 using the stereotactic coordinates: −1.80 mm posterior to bregma, ±1.50 mm lateral to midline, −1.60 mm ventral to skull surface; −2.50 mm posterior to bregma, ±2.00 mm lateral to midline, −1.70 mm ventral to skull surface.

Drug injections. Clozapine-*N*-oxide (CNO; Enzo Life Sciences) was made in a stock solution of 0.5 mg ml^{-1} in DMSO and then diluted in saline to desired concentration. CNO was injected (i.p.) at a dose of 0.5 mg kg^{-1} 45 min before behavioural manipulation. MK-801 (Sigma-Aldrich) was diluted in saline and injected (i.p.) at a dose of 0.1 mg ml^{-1} 30 min before behavioural manipulation. Saline was used as the vehicle.

Behavioural procedures. Prior to all experiments, mice were handled for one minute in the vivarium each day for three days. Then, mice were habituated to transportation and external environmental cues by being carted out of the vivarium into the experimental rooms and handled for one minute in the experimental room each day for five days before the experiment. For within-subject experiments, mice explored three different contexts, separated by 7 days or 5 hours. Exploration duration of each context was ten minutes (C57Bl/6NTac and C57Bl/6NIA strains) or five minutes (C57Bl/6NTac × 129S6/SvEvTac strain). Contexts were counterbalanced. For between-subject experiments, mice explored two contexts separated by either 7 days or 5 h. The area of each context was approximately 800 cm^2. The shape (circular, triangular, square), scent (simple green, omega, alcohol), visual cues (white plastic walls/opaque textured flooring, black acrylic walls/white acrylic flooring, metal walls/metal grid flooring) were different for each context. For immediate shock[31] (imm shock), mice were placed in the chamber with a baseline of 10 s (0.7 mA) (C57Bl/6NTac and C57Bl/6NIA strains) or 6 s (C57Bl/6NTac × 129S6/SvEvTac strain) followed by a 2 s shock (0.7 mA, C57Bl/6NTac and C57Bl/6NIA strains; 0.5 mA, C57Bl/6NTac × 129S6/SvEvTac strain). Thirty seconds after the shock, mice were placed back in their home cage. For context tests (cxt test), mice were returned to the designated context. For extinction (extinct) trials, mice were placed in a context for five minutes without shock. Freezing (the cessation of all movement except for respiration), was assessed via an automated scoring system (Med Associates) with 30 frames per second sampling; the mice needed to freeze continuously for at least one second before freezing could be counted[32,33]. Experimental groups and contexts were counterbalanced across the within-subjects design. For between-subjects design, animals were randomly assigned to groups.

Integrated miniature microscope data acquisition and analyses. Digital imaging data was sent from the CMOS imaging sensor (Aptina, MT9V032) to custom data acquisition (DAQ) electronics and USB host controller (Cypress, CYUSB3013) over a lightweight, highly flexible cable. The electronics packaged the data to comply with the USB video class (UVC) protocol and then transmit the data over Super Speed USB to a PC running custom DAQ software. The DAQ software was written in C++ and uses Open Computer Vision (OpenCV) libraries for image acquisition. Images are acquired at 30 frames per second and recorded to uncompressed .avi files. The DAQ software simultaneously records animal behaviour, time stamping both video streams for offline alignment.

Our analysis suite, written in MATLAB, processes the raw videos and extracts relevant experimental information. Initial processing of calcium imaging data corrected column-wise ADC variation, removed small movement artefacts using an amplitude-based image registration algorithm, and calculated the mean fluorescence per pixel for conversion to $\Delta F/F$. A fully automated segmentation algorithm identified and segmented pixels of active cells. The algorithm steps through the recorded calcium imaging video detecting pixel locations of local maxima of fluorescence which met a minimum $\Delta F/F$ criteria. For each of these pixel locations, an iterative process was used to group together neighbouring pixels based on that pixel's fluorescence time trace (±5 s window around local maxima of fluorescence event) correlation with the mean time trace of the pixels group in the previous iterative step. Pixels with high correlation (0.95) were added to the group and the process was repeated until the total number of pixels in the group no longer changed. Cells whose centres were within 7 μm of each other or whose pixels overlapped by at least 80% were merged together. Once cells were segmented, we extracted $\Delta F/F$ traces and removed crosstalk between neighbouring cells. Crosstalk was removed by first detecting calcium transients across all cells and then keeping only the largest event within a 30 μm radius of the cell they were associated with[7]. Calcium events were calculated by first filtering the $\Delta F/F$ (2-pole Butterworth low-pass filter: 0.3 Hz) to remove noise. Peaks in the filtered $\Delta F/F$ trace above 0.05 $\Delta F/F$ were detected and a window was calculated from the onset of the peak to the return back to baseline. If this window was greater than one second, it was counted as an event. Recordings from multiple sessions of the same animal were aligned using the same amplitude-based registration algorithm used for within-session registration, except the algorithm was only applied to the mean frame from each session. Once two sessions were registered, cells across two sessions were matched to each other using a distance measure (centres within 5 μm of each other).

Code availability. The MATLAB analysis suite, as described above, is available for download at http://www.miniscope.org. This Wiki site is our open-source platform for sharing access to all of our associated software and hardware files for implementing our miniature microscope.

Confocal imaging and histological analysis. Forty-five minutes after exploration of a context, mice were transcardially perfused with 4% PFA, followed by 24 h post-fixation in the same solution. Free-floating 50-μm coronal sections were prepared using a vibratome. Sections were incubated in blocking solution containing 0.2% Triton X, 10% normal goat serum in 0.1 M phosphate buffer for at least 1 h at room temperature. Then the sections were incubated in the blocking solution with anti-EGR-1 rabbit primary antibody (Cell Signaling; 1:750 dilution for 24 h at 4 °C). After a series of 0.1 M phosphate buffer washes, sections were stained using the same blocking solution as above and Alexa Fluor 568 goat anti-rabbit secondary antibody (Jackson Immuno Research; 1:500 dilution for 2 h at room temperature).

Finally, sections were stained with DAPI (Invitrogen; 1:1,000 dilution for 15 min) and mounted on slides.

Sections from −1.8 mm to −2.2 mm posterior to bregma were imaged at 20× magnification using a Nikon C2 or A1 confocal microscope. All imaging was done using standardized laser settings, held constant for samples from the same experimental data set. Cells were manually counted by a blinded rater. Images were quantified from 1–4 sections per animal. The percentage of DAPI-labelled cells containing GFP, ZIF, or both was calculated for each image and then averaged to produce a single measurement for each animal. To normalize for chance, we subtracted chance (GFP/DAPI) × (ZIF/DAPI) × 100 from the observed overlap (GFP and ZIF)/DAPI × 100 and then divided by chance.

Electrophysiology. Mice were anaesthetized with a cocktail (3 ml kg^{-1}) containing ketamine (25 mg ml^{-1}), xylazine (1.3 mg ml^{-1}), and acepromazine (0.25 mg ml^{-1}) and perfused for 3 min with ice-cold, oxygenated, sucrose ACSF containing (in mM) 83 NaCl, 2.5 KCl, 3.3 $MgSO_4$, 0.5 $CaCl_2$, 1 NaH_2PO_4, 26.2 $NaHCO_3$, 22 glucose, and 72 sucrose (~315 mOsml, pH 7.4). The brain was rapidly dissected and 300-μm-thick coronal slices were collected and transferred to an interface chamber containing the same modified sucrose ACSF solution and incubated at 34 °C for 30 min. Slices were then held at room temperature (23 °C) in the interface chamber for at least 45 min before initiating recordings. Recordings were made in a submersion-type recording chamber and perfused with oxygenated ACSF containing (in mM) 119 NaCl, 2.5 KCl, 1.3 $MgCl_2$, 2.5 $CaCl_2$, 1.3 NaH_2PO_4, 26.0 $NaHCO_3$, 20 glucose (~295 mOsml) at 23 °C at a rate of 1–2 ml per minute.

All recordings were performed within the CA1 region of the hippocampus. Neurons were selected based on emission spectra (GFP^+ or GFP^-), and were then visualized under infrared differential interference contrast video microscopy (Olympus BX-51 scope and Rolera XR digital camera). Whole-cell recordings were made at room temperature using pulled patch pipettes (5–6 MΩ) filled with internal solution containing (in mM) 150 K-Gluconate, 1.5 $MgCl_2$, 5.0 HEPES, 1 EGTA, 10 phosphocreatine, 2.0 ATP, and 0.3 GTP. Recordings were obtained using Multiclamp 700B patch amplifiers (Molecular Devices) and data analysed using pClamp 10 software (Molecular Devices). Data were acquired from cells requiring less than −100 pA to hold at a membrane potential of −70 mV. Current–spike relationship was determined with a series of depolarizing current steps applied for 500 ms in 10 pA increments at 5 s intervals.

Statistical analysis. GraphPad Prism version 6.00 (GraphPad Software, La Jolla, California, USA) was used for statistical analyses. Statistical significance was assessed by two-tailed paired Student's *t*-tests, two-tailed unpaired Student's *t*-tests, one-way ANOVA, or two-way ANOVA where appropriate. Significant effects or interactions were followed up with post hoc testing with the use of Fisher's least significant difference (LSD) where specified in the figure legends. Significance levels were set to $P = 0.05$. Significance for comparisons: $^*P < 0.05$; $^{**}P < 0.01$; $^{***}P < 0.001$. Sample sizes were chosen on the basis of previous studies. No statistical methods were used to predetermine sample size. Data met assumptions of statistical tests, and variance was similar between groups for all metrics measured. The investigators were blinded to conditions and drugs during experiments and outcome assessment.

30. Sano, Y. *et al.* CREB regulates memory allocation in the insular cortex. *Curr. Biol.* **24,** 2833–2837 (2014).
31. Frankland, P. W. *et al.* Consolidation of CS and US representations in associative fear conditioning. *Hippocampus* **14,** 557–569 (2004).
32. Anagnostaras, S. G. *et al.* Automated assessment of pavlovian conditioned freezing and shock reactivity in mice using the video freeze system. *Front. Behav. Neurosci.* **4,** 158 (2010).
33. Cai, D. J., Shuman, T., Gorman, M. R., Sage, J. R. & Anagnostaras, S. G. Sleep selectively enhances hippocampus-dependent memory in mice. *Behav. Neurosci.* **123,** 713–719 (2009).

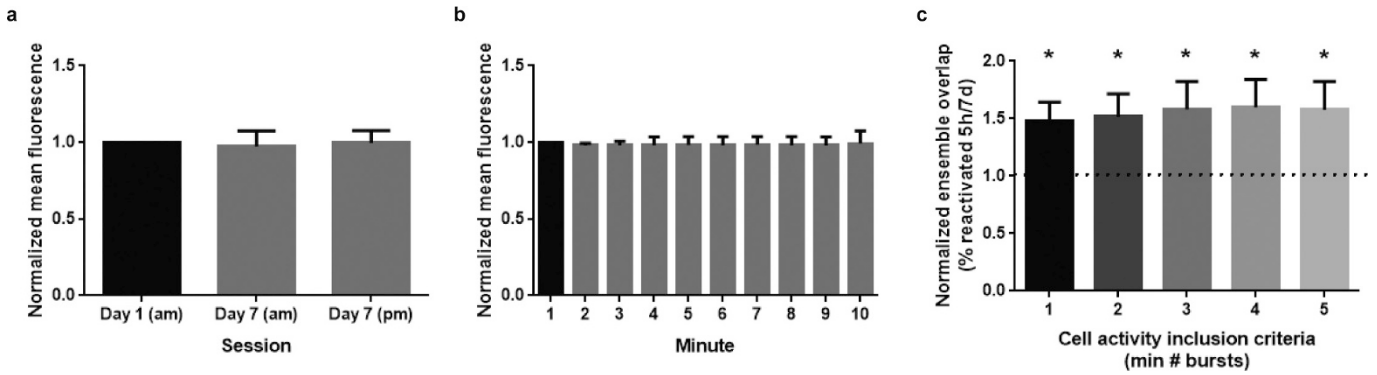

Extended Data Figure 1 | Stability of fluorescence and overlap. **a**, Average normalized mean fluorescence within session. There was no difference between the mean fluorescence across the 3 sessions (one-way repeated measures ANOVA, $F_{2,7} = 0.423$, not significant). **b**, Average normalized mean fluorescence within session. There was no difference between the mean fluorescence across a 10-min session (one-way repeated measures ANOVA, $F_{9,22} = 1.108$, not significant). Results show mean ± s.d. **c**, Higher ensemble overlap with 5 h interval than 7 days. Normalized ensemble overlap is calculated as the ensemble overlap between contexts separated by 5 h divided by the ensemble overlap between contexts separated by 7 days. A normalized overlap value of 1 signifies that there is no difference between the overlap at 5 h and 7 days. The minimum number of calcium events required from each cell for the cell to be considered 'active' (inclusion criteria) was systematically increased and the ratio of the ensemble overlap for the different context was calculated. For all inclusion criteria, there is higher ensemble overlap with a 5 h, rather than 7 day, interval (one-sample *t*-test against 1, (1) $t_7 = 3.00$, $P = 0.02$, (2) $t_7 = 2.57$, $P = 0.04$, (3) $t_7 = 2.42$, $P = 0.04$, (4) $t_7 = 2.50$, $P = 0.04$, (5) $t_7 = 2.32$, $P = 0.05$). Results show mean ± s.e.m.

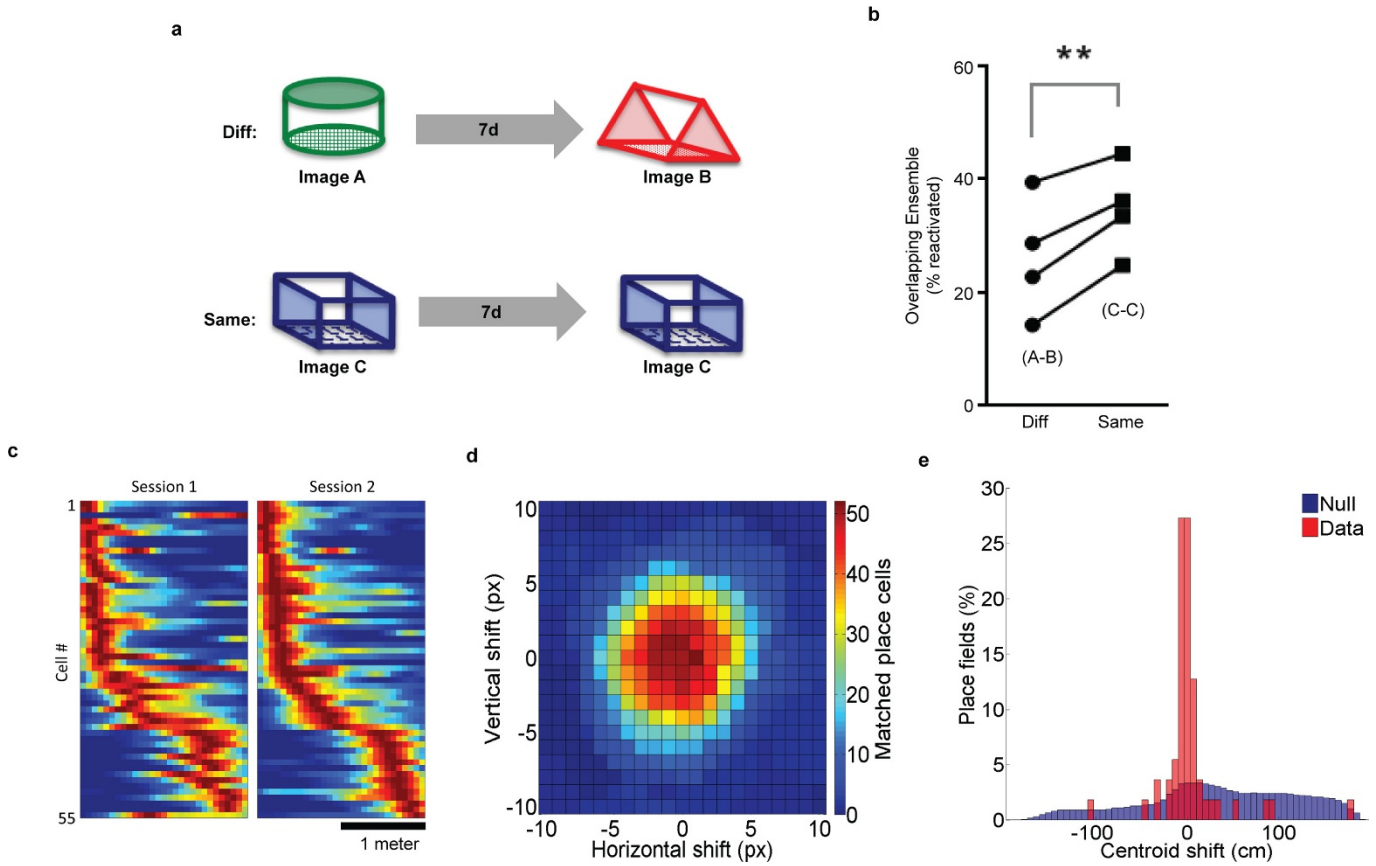

Extended Data Figure 2 | Neural ensembles of environments are reliably reactivated at recall of an open field and linear track. a, Experimental design. Mice were imaged while exploring contexts A and B separated by 7 days and imaged while exploring contexts C and C separated by 7 days. **b**, There was a higher percentage of cells reactivated when animals explored the same context (C–C) than when animals explored different contexts (A–B) (paired *t*-test, $t_3 = 6.305$, $P = 0.0081$, $n = 4$ mice). **c**, Mice were trained to run on a 2-m linear track with the miniature microscope for water rewards. Mice were trained 3 days a week for 3 weeks with a delay interval of 2–3 days between each session. Place fields were calculated by deconvolving calcium $\Delta F/F$ traces with an exponential to extract approximate spike times. Spikes that remained after crosstalk removal were included for analysis. Animal position was extracted using an automated LED tracking algorithm. A speed threshold (3 cm s^{-1}) was applied to both the animal position and extracted spike timing and the resulting data was spatially binned (6.5-cm bins). Spatial firing rates were calculated by dividing the binned spike counts by the binned occupancy and smoothing with a Gaussian filter (sigma = 6.5 cm). Cells which showed consistent spatial firing modulation on at least three trials, with all other trials showing no bursting activity, were considered as place cells. Normalized spatial firing rates of all matched cells independently meeting the place cell criteria for both days. The data are pooled across 3 mice and include both motion directions. Place fields are ordered by centroid location on session 2. **d**, A shift of the image registration between sessions results in a decrease in matched place cells. A translational shift both horizontally and vertically was applied to the image registration transformation used in A. Cells were then matched across days and those which met our place cell criteria were kept. The heat map shows the count of matched place cells with a centroid shift of the place field that is less than 33 cm. Optimum matching of cells occurred within a 1-pixel translation of the calculated alignment transformation. **e**, Distribution of centroid shifts of place fields shown in A compared to the null hypothesis that the cell matching between sessions matches random cells.

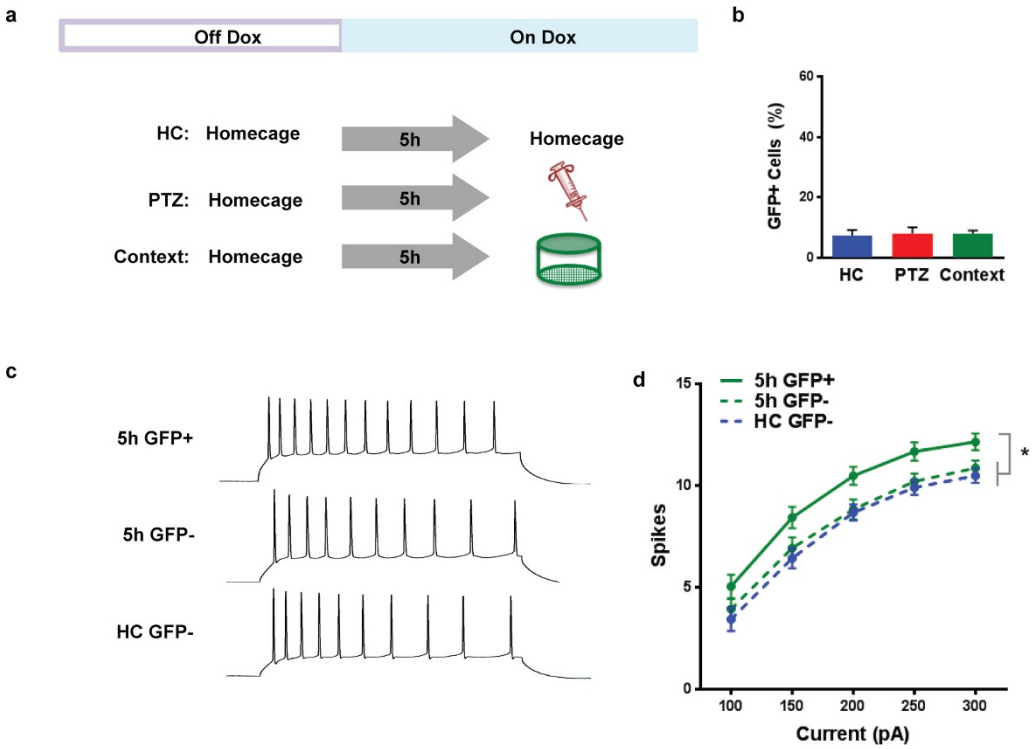

Extended Data Figure 3 | Five hours after exploration of a context, GFP expression is shut off by doxycycline and excitability is increased. **a**, Experimental design. Mice were removed from low levels of dox (40 mg kg^{-1}) and given regular chow for 3 days to open up the GFP tagging window. After receiving administration of high dox (1 g kg^{-1}) for 5 h, mice were injected with 30 mg kg^{-1} of pentylenetetrazole (PTZ), exposed to a novel context or left in their home cage (HC). An hour later, mice were transcardially perfused and processed for GFP expression. **b**, There was no difference in GFP expression between the three groups (one-way ANOVA, $F_{2,5} = 0.04$, not significant, $n = 3, 3, 2$ mice), demonstrating that 5 h was enough time for dox (1 g kg^{-1}) to suppress expression of new GFP. **c**, To test excitability learning-related excitability changes, mice explored a novel context and then were administered high dox to shut off new GFP. Five hours later, mice were euthanized for *in vitro* slice physiology. **d**, A two-way repeated measures ANOVA (group × current step) had a significant main effect of group ($F_{2,68} = 4.20$, $P < 0.05$, $n = 21, 29, 21$ cells). The 5 h GFP$^+$ group had more spikes than the 5 h GFP$^-$ group ($t_{68} = 2.31$, $P < 0.05$) and home cage GFP$^-$ ($t_{68} = 2.72$, $P < 0.05$). There was no difference between the 5 h GFP$^-$ and home cage GFP$^-$ groups ($t_{68} = 0.61$, not significant). Results show mean ± s.e.m.

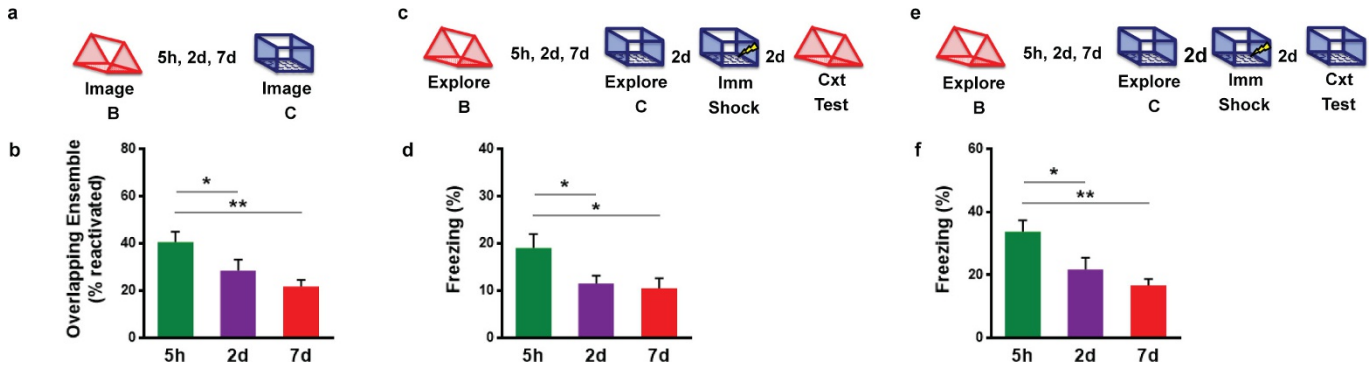

Extended Data Figure 4 | Time course for neuronal overlap and behavioural linking. a, Design for Ca^{2+} imaging of neuronal overlap experiment. **b**, There was a significant difference in overlap across groups (one-way repeated measures ANOVA, $F_{2,12} = 12.43$, $P = 0.002$, $n = 7$ mice). There was more overlap at 5 h than 2 days ($t_{12} = 3.03$, $P = 0.01$) and 7 days ($t_{12} = 4.72$, $P = 0.0005$). **c**, Design for transfer of fear experiment. **d**, There was a significant difference in freezing across groups (one-way ANOVA, $F_{2,43} = 3.55$, $P = 0.04$, $n = 20$, 14, 12 mice). There was more freezing at 5 h than 2 days ($t_{43} = 2.13$, $P = 0.04$) and 7 days ($t_{43} = 2.31$, $P = 0.03$). **e**, Design for enhancement experiment. **f**, There was a significant difference in freezing across groups (one-way ANOVA, $F_{2,45} = 6.38$, $P = 0.004$, $n = 22$, 14, 12 mice). There was more freezing at 5 h than 2 days ($t_{45} = 2.45$, $P = 0.02$) and 7 days ($t_{45} = 3.32$, $P = 0.002$). Results show mean ± s.e.m.

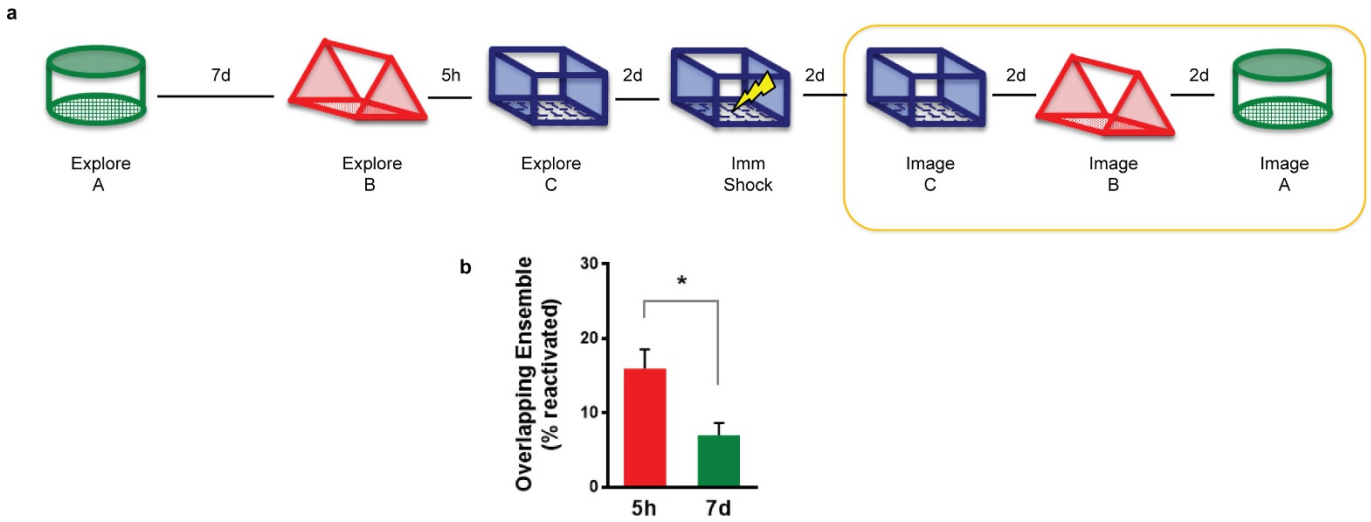

Extended Data Figure 5 | Calcium imaging during retrieval. a, Design for Ca^{2+} imaging of neuronal overlap at retrieval. Order of contexts during retrieval was counterbalanced. **b**, There was higher overlap of the neuronal ensemble at 5 h than 7 days (paired *t*-test, $t_7 = 2.55$, $P = 0.04$, $n = 8$ mice). Results show mean ± s.e.m.

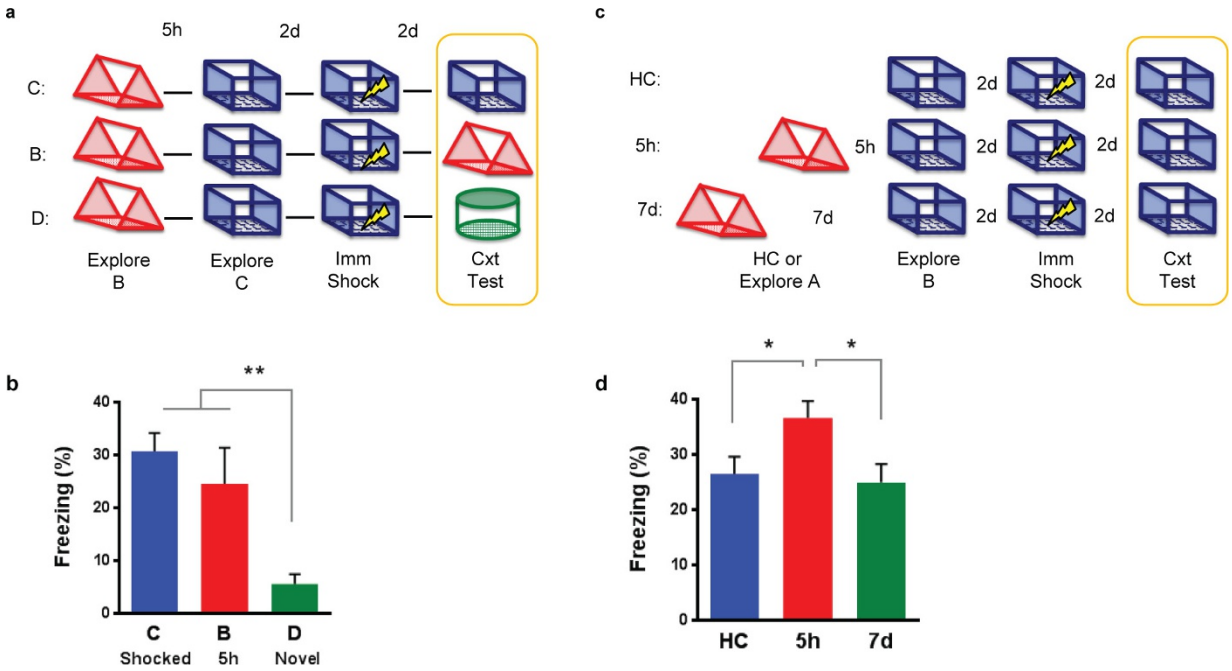

Extended Data Figure 6 | Replication of memory linking experiments in young (3–6 months old) C57Bl/6NIA mice. a, Design for transfer of fear experiment. **b**, There was a significant difference in freezing across the groups (one-way ANOVA, $F_{2,20} = 9.49$, $P = 0.001$, $n = 8, 7, 8$ mice). There was no difference between freezing levels in context C or B ($t_{20} = 0.99$, not significant). Animals had less freezing in context D than C ($t_{20} = 4.19$, $P = 0.0004$) and B ($t_{20} = 3.06$, $P = 0.006$). **c**, Design for enhancement experiment. **d**, There was a significant difference in freezing (one-way ANOVA, $F_{2,46} = 4.071$, $P = 0.023$, $n = 16, 17, 16$ mice). The 5 h group had more freezing than the home cage (HC) group ($t_{46} = 2.72$, $P = 0.0278$) and 7 day group ($t_{46} = 2.612$, $P = 0.012$). There was no difference between home cage or 7 day groups ($t_{46} = 0.335$, not significant). Results show mean ± s.e.m.

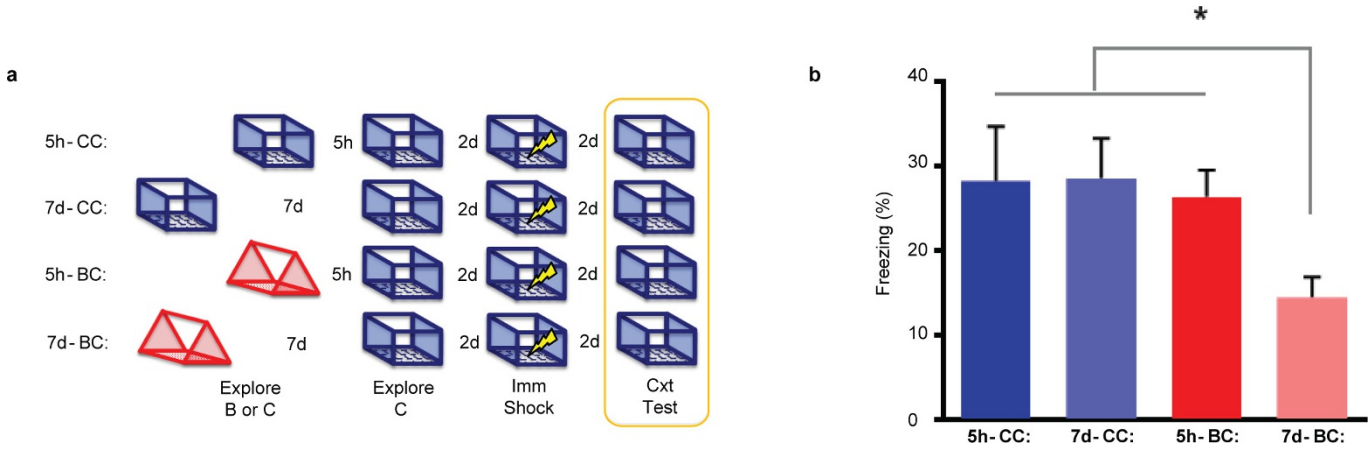

Extended Data Figure 7 | Exploring the same context twice enhances memory regardless of time. a, Experimental design. **b**, There was a significant difference in freezing (one-way ANOVA, $F_{3,44} = 2.92$, $P = 0.04$, $n = 10, 11, 13, 14$ mice). Consistent with the prior experiment, there was more freezing in the 5 h BC than the 7 day BC group ($t_{44} = 2.19$, $P < 0.05$). The 7 day BC group also had more freezing than the 5 h CC ($t_{44} = 2.35$, $P < 0.05$) and 7 day CC ($t_{44} = 2.48$, $P < 0.05$) groups, however there were no difference between the 5 h CC and 7 day CC ($t_{44} = 0.06$, not significant) and 5 h CC and 5 h BC ($t_{44} = 0.31$, not significant) groups. Results show mean ± s.e.m.

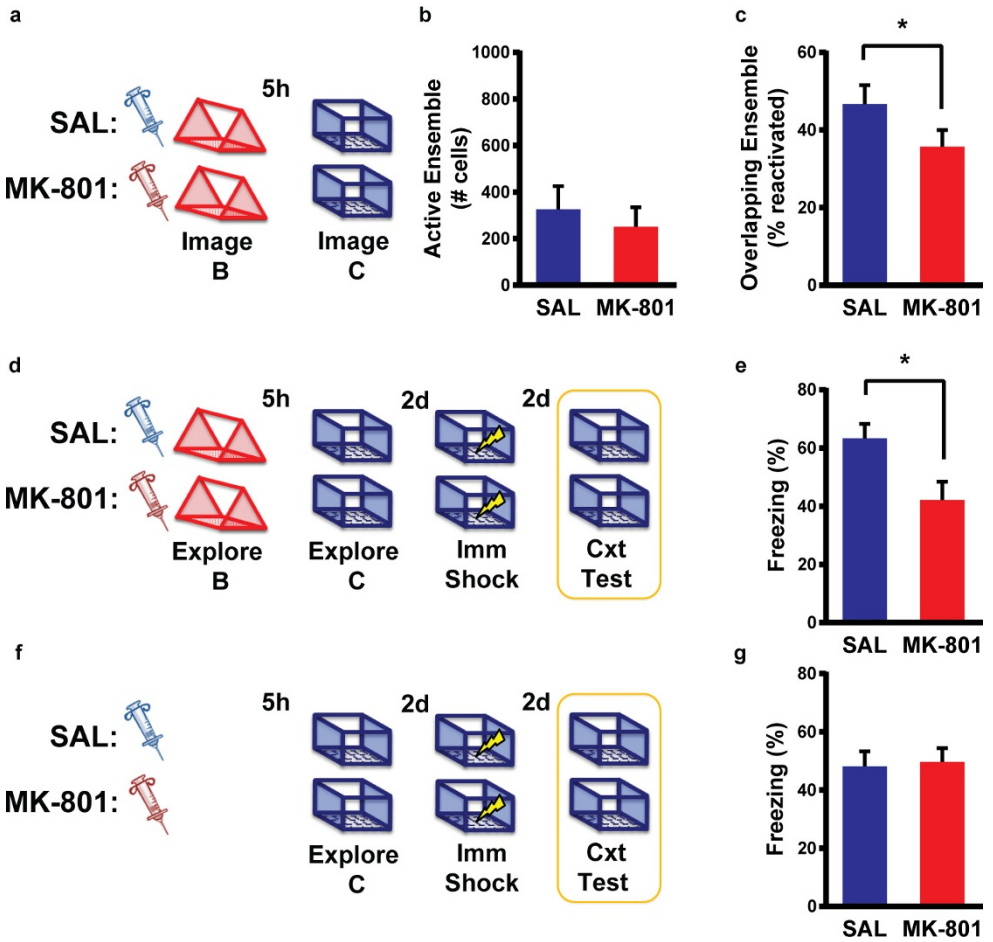

Extended Data Figure 8 | NMDA receptor activity is required for overlap of neural ensembles and behavioural enhancement. a, Design for Ca^{2+} imaging of neuronal overlap with MK-801 or saline. **b**, There was no difference in the number of cells active during exploration of the first context between saline-injected (SAL) and MK-801 groups (unpaired *t*-test, $t_6 = 0.58$, not significant, $n = 4, 4$). **c**, There was lower overlap of the neuronal ensemble in the MK-801 group than in the SAL group (paired *t*-test, $t_3 = 3.45$, $P = 0.04$, $n = 4$ mice). **d**, Design for behavioural enhancement experiment. **e**, There was lower freezing in the MK-801 than in the SAL group (unpaired *t*-test, $t_{22} = 2.65$, $P = 0.015$, $n = 12, 12$ mice). **f**, Design for behavioural control experiment. **g**, There was no difference in freezing between SAL and MK-801 groups (unpaired *t*-test, $t_{22} = 0.22$, not significant, $n = 12, 12$ mice). Results show mean ± s.e.m.

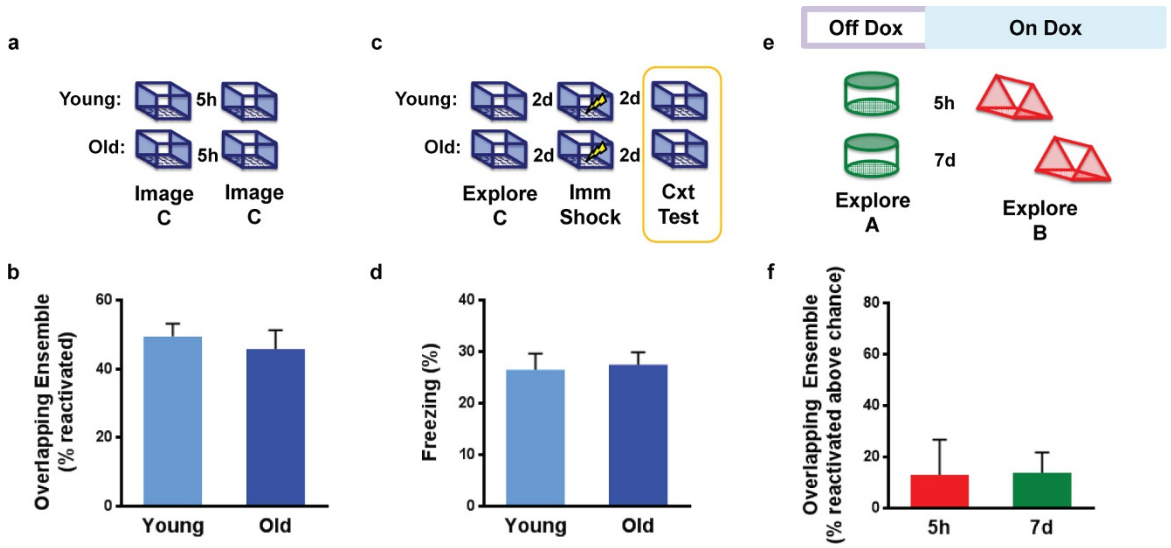

Extended Data Figure 9 | Control experiments for aged mice. a, Design for experiment of recall for single contextual experience. **b**, There was no difference in reactivation of cells between young and old mice during recall (unpaired *t*-test, $t_6 = 0.59$, not significant, $n = 4$, 4 mice). **c**, Design for experiment with single context pre-exposure in young and old mice. **d**, There was no difference in freezing behaviour to exposures of a single context (unpaired *t*-test, $t_{29} = 0.24$, not significant, $n = 16$, 15 mice). **e**, Design for replication of TetTag experiment in old mice. **f**, There was no difference in the levels of overlapping ensembles between the 5 h and 7 day groups (unpaired *t*-test, $t_6 = 0.06$, not significant, $n = 3$, 5 mice). Results show mean ± s.e.m.

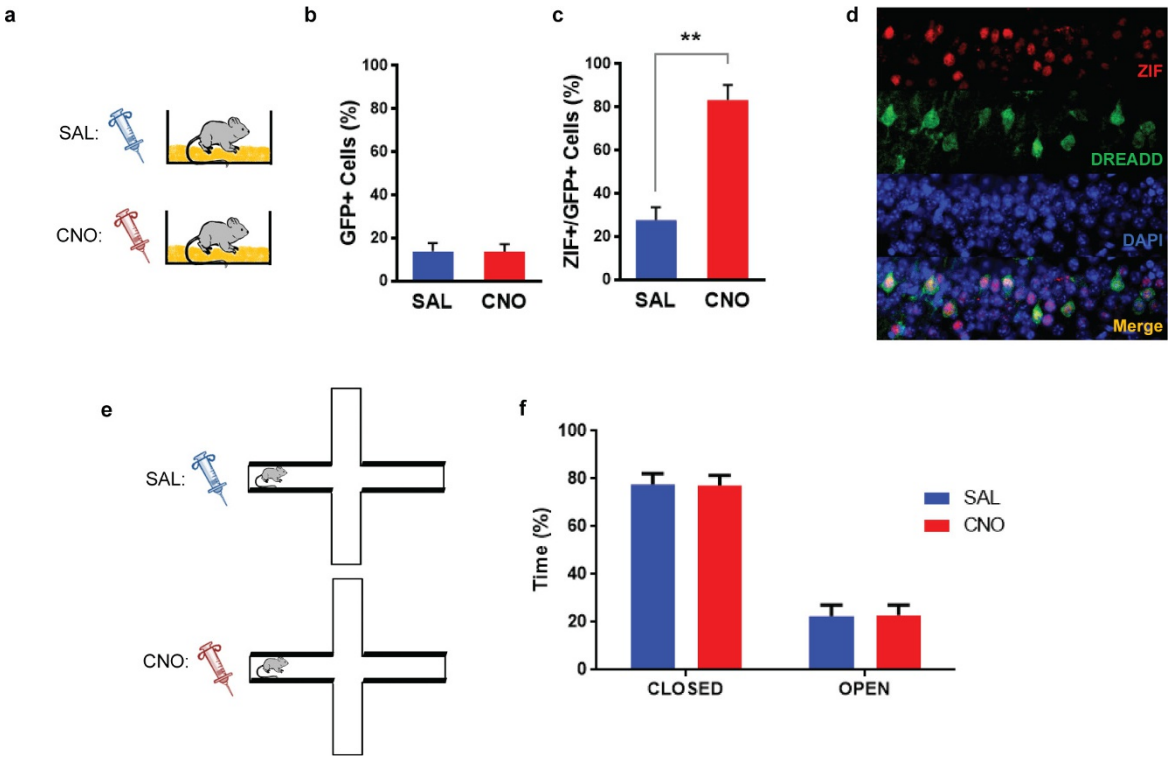

Extended Data Figure 10 | CNO activates cells with DREADD receptors and does not increase anxiety in aged mice. a, Mice infected with DREADD virus in CA1 were injected with saline (SAL) or clozapine-*N*-oxide (CNO) and then euthanized 90 min post-injection for immunofluorescence staining. **b**, There was no difference in the percentage of DREADD-positive cells (labelled with GFP) between SAL and CNO groups (unpaired *t*-test, $t_7 = 0.01$, not significant, $n = 3, 6$ mice). **c**, DREADD-positive cells (labelled with GFP) had more ZIF when injected with CNO than SAL (unpaired *t*-test, $t_7 = 5.08$, $P = 002$). **d**, Representative examples of ZIF, DREADD, DAPI as well as merged images of CA1. **e**, Design for elevated plus maze experiment in aged mice with DREADD virus. **f**, A two-way ANOVA showed no main effect of injection ($F_{1,9} = 0.75$, not significant, $n = 6$, 5 mice) and a significant main effect of arms ($F_{1,9} = 71.03$, $P < 0.0001$). There was no significant interaction between injection and arms ($F_{1,9} = 0.003$, not significant). Results show mean ± s.e.m.